Inorganic Chemistry Communications 27 (2013) 13–17

Contents lists available at SciVerse ScienceDirect

Inorganic Chemistry Communications

journal homepage: www.elsevier.com/locate/inoche

An organic–inorganic hybrid 1-D double-chain copper–yttrium heterometallic silicotungstate $[Cu(dap)_2(H_2O)]_2\{Cu(dap)_2[\alpha\text{-}H_2SiW_{11}O_{39}Y(H_2O)_2]_2\}\cdot 10H_2O$

Jie Luo [a], Junwei Zhao [a,b,*], Jing Yuan [a], Yanzhou Li [a], Lijuan Chen [a,c], Pengtao Ma [a], Jingping Wang [a], Jingyang Niu [a,**]

[a] Institute of Molecular and Crystal Engineering, College of Chemistry and Chemical Engineering, Henan University, Kaifeng, Henan 475004, P. R. China
[b] State Key Laboratory of Structural Chemistry, Fujian Institute of Research on the Structure of Matter, Chinese Academy of Sciences, Fuzhou, Fujian 350002, P. R. China
[c] Basic Experiment Teaching Center, Henan University, Kaifeng, Henan 475004, P. R. China

ARTICLE INFO

Article history:
Received 27 August 2012
Accepted 9 October 2012
Available online 17 October 2012

Keywords:
Polyoxometalate
Silicotungstate
Copper–yttrium heterometal
1-D double-chain structure

ABSTRACT

An organic–inorganic hybrid 1-D double-chain Cu^{II}–Y^{III} heterometallic silicotungstate $[Cu(dap)_2(H_2O)]_2\{Cu(dap)_2[\alpha\text{-}H_2SiW_{11}O_{39}Y(H_2O)_2]_2\}\cdot 10H_2O$ (**1**) has been synthesized by reaction of $Na_{10}[A\text{-}\alpha\text{-}SiW_9O_{34}]\cdot 18H_2O$, $CuCl_2\cdot 2H_2O$, YCl_3 and dap (dap = 1,2-diaminopropane) under hydrothermal conditions and characterized by elemental analyses, IR spectrum, UV spectrum and single-crystal X-ray diffraction. **1** exhibits a novel 1-D double-chain structure constructed from dimeric Cu^{II}–Y^{III} heterometallic silicotungstate units. To our knowledge, **1** is the first organic–inorganic hybrid 1-D double-chain Cu^{II}–Y^{III} heterometallic polyoxometalate. Thermogravimetry-differential thermal analysis of **1** has been measured from 25 to 750 °C and the thermogravimetric curve indicates two steps of weight loss.

Polyoxometalates (POMs), as a typical class of metal–oxo clusters with oxygen-enriched surfaces, have attracted considerable interest owing to their diverse compositional and structural varieties, extensive electronic versatility and intriguing properties in catalysis, magnetism, electrochemistry and materials science [1–5]. Within this field, lacunary POM segments can integrate various transition-metal (TM) or rare-earth (RE) cations, which have led to a large number of TM or RE substituted POMs [6–12]. With the rapid development of POM chemistry and the interpenetrating trend of multidisciplinarities, the design and synthesis of POM-based TM–RE heterometallic derivatives (TRHDs) has gradually become an emerging field of research. Because there is an unavoidable competitive reaction among highly negative POM precursors, strongly oxyphilic RE cations and less active TM cations in the same reaction system [13], currently, exploring and discovering novel POM-based TRHDs with interesting structures and properties remains a severe and longstanding challenge. Albeit some similar species have been successively synthesized [14–20], such as $[\{RE(PW_{11}O_{39})_2\}\{Cu_2(bpy)_2(\mu\text{-}ox)\}]^{9-}$ (RE = La^{III}, Pr^{III}, Eu^{III}, Gd^{III}, Yb^{III}) (bpy = 2,2′-bipyridine, ox = oxalate) [14], $[K\subset\{FeCe(AsW_{10}O_{38})(H_2O)_2\}_3]^{14-}$ [13], $[\{\alpha\text{-}P_2W_{15}O_{56}\}_6\{Ce_3Mn_2(\mu_3\text{-}O)_4(\mu_2\text{-}OH)_2\}_3(\mu_2\text{-}OH)_2(H_2O)_2(PO_4)]^{47-}$ [15], $[K_3\subset\{GdCo(H_2O)_{11}\}_2\{P_6W_{41}O_{148}(H_2O)_7\}]^{13-}$ [16], $\{[Ce_3Mn_2O_6(OAc)_6(H_2O)_9]_2[Mn_2P_2W_{16}O_{60}]_3\}^{20-}$ (OAc = CH_3COO^-) [17], $[K\subset K_7Ce_{24}Ge_{12}W_{120}O_{456}(OH)_{12}(H_2O)_{64}]^{52-}$ [18], $[\{CuTbL(H_2O)_2\}_2\{AlMo_6O_{18}(OH)_6\}_2]\cdot MeOH\cdot 10H_2O$ (L = N,N′-bis(3-methoxysalicylidene)ethylenediamine) [19], $\{[Cu(dap)_2]_{4.5}[Dy(\alpha\text{-}PW_{11}O_{39})_2]\}^{2-}$ [20], $\{[Cu(en)_2]_{1.5}[Cu(en)(2,2'\text{-}bipy)(H_2O)_n]RE[(\alpha\text{-}PW_{11}O_{39})_2]\}^{6-}$ (RE = Ce^{III}, Pr^{III}) [21] and $\{[Cu(en)_2(H_2O)][Cu_3RE(en)_3(OH)_3(H_2O)_2](\alpha\text{-}GeW_{11}O_{39})\}_2$ (RE = Eu^{III}, Tb^{III}, Dy^{III}) [22] since the first POM-based TRHD $[((VO)_2Dy(H_2O)_4K_2(H_2O)_2Na(H_2O)_2)(B\text{-}\alpha\text{-}AsW_9O_{33})_2]^{8-}$ was discovered in 2007 [23]. To date, investigations on silicotungstate(ST)-based TRHDs remain less explored [24–29], which provides us a good opportunity to exploit this field. In 2007–2011, Wang *et al.* reported several ST-based TRHDs $[\{Ce(H_2O)_7\}_2Mn_4Si_2W_{18}O_{68}(H_2O)_2]^{6-}$ [24], $\{Nd_2(H_2O)_{12}Cu_4(H_2O)_2(SiW_9O_{34})_2\}^{6-}$ [25] and $[K_9RE_6Fe_6(H_2O)_{12}(SiW_{10}O_{38})_6]^{26-}$ (RE = Dy^{III}, Tb^{III}) [26]. In 2009–2010, Mialane et al. communicated the $\{RECu_3(OH)_3O\}$-cubane inserted STs $\{[Cu(en)_2(H_2O)][(Cu(en)(OH))_3RE(SiW_{11}O_{39})(H_2O)]\}_2\cdot 20H_2O$ (RE = La^{III}, Gd^{III}, Eu^{III}) and a 1D double-chain $[(\gamma\text{-}SiW_{10}O_{36})_2(Cr(OH)(H_2O))_3(La(H_2O)_7)_2]^{4-}$ [27,28]. In 2010, Su and coworkers isolated ST-based TRHDs with mixed organic ligands $[Cu(en)_2H_2O]_3[(\alpha\text{-}SiW_{11}O_{39})RE(H_2O)(\eta^2,\mu\text{-}1,1)\text{-}CH_3COO]$ (RE = Nd^{III}, Sm^{III}) [29]. Recently, our group have launched the investigations on the reactions of $K_4[\alpha\text{-}SiW_{12}O_{40}]\cdot 17H_2O$ with Cu – RE heterometal cations and a class of ST-based TRHD hybrids $\{[Cu(en)_2]_{1.5}RE[(\alpha\text{-}SiW_{11}O_{39})_2]\}_2^{20-}$ (RE = Gd^{III}, Tb^{III}, Dy^{III}, Er^{III}, Lu^{III}) [30] and $[Cu(en)_2(H_2O)]_2\{[Cu(en)_2][Cu(en)_2(H_2O)][(\alpha\text{-}SiW_{11}O_{39})RE(H_2O)(pzda)]\}_2^{2-}$ (RE = Y^{III}, Dy^{III}, Yb^{III}, Lu^{III}) [31] have been isolated. Very recently, we have expanded our study to the system containing $Na_{10}[\alpha\text{-}SiW_9O_{34}]\cdot 18H_2O$, $CuCl_2\cdot 2H_2O$, $RECl_3$ and dap under

* Correspondence to: J. Zhao, Institute of Molecular and Crystal Engineering, College of Chemistry and Chemical Engineering, Henan University, Kaifeng, Henan 475004, P. R. China. Tel./fax: +86 378 3886876.
** Corresponding author. Tel./fax: +86 378 3886876.
E-mail addresses: zhaojunwei@henu.edu.cn (J. Zhao), jyniu@henu.edu.cn (J. Niu).

1387-7003/$ – see front matter © 2012 Elsevier B.V. All rights reserved.
http://dx.doi.org/10.1016/j.inoche.2012.10.014

hydrothermal conditions based on the following considerations: (a) The accessible trivacant Keggin-type $[A\text{-}\alpha\text{-}SiW_9O_{34}]^{10-}$ precursor offers us the ample starting material to prepare ST-based TRHDs; (b) compared with other TM cations, Cu^{II} ions exhibit more flexible various coordination modes (square, trigonal bipyramid, square pyramid and octahedron), moreover, the Jahn–Teller effect of the octahedron and pseudo-Jahn–Teller effect of the square pyramid for Cu^{II} cations can make them adopt diverse linking modes to overcome steric hindrance and then form novel architectures; (c) Because combination of RE cations with lacunary STs often leads to precipitation, the hydrothermal method has been utilized to enhance the solubility of the reactants. Thus, three hybrid ST-based TRHDs $NaH[Cu(dap)_2(H_2O)][Cu(dap)_2]_{4.5}[RE(\alpha\text{-}SiW_{11}O_{39})_2]\cdot 7H_2O$ ($RE = Sm^{III}$, Dy^{III}, Gd^{III}) have been afforded [32]. As our continuous work, an organic–inorganic hybrid ST-based TRHD $[Cu(dap)_2(H_2O)]_2\{Cu(dap)_2[\alpha\text{-}H_2SiW_{11}O_{39}Y(H_2O)_2]_2\}\cdot 10H_2O$ (**1**) has been obtained and characterized by elemental analyses, IR spectrum, UV spectrum, thermogravimetry–differential thermal analysis and single-crystal X-ray diffraction. As far as we know, it is the first organic–inorganic hybrid 1-D double-chain Cu^{II}–Y^{III} heterometallic POM.

1 was hydrothermally prepared by a mixture of $Na_{10}[A\text{-}\alpha\text{-}SiW_9O_{34}]\cdot 18H_2O$ (0.140 g, 0.050 mmol), $CuCl_2\cdot 2H_2O$ (0.140 g, 0.821 mmol), YCl_3 (0.051 g, 0.261 mmol), dap (0.20 mL, 1.801 mmol), H_2O (5 mL, 278 mmol) and HCl (0.30 mL, 2 mol L^{-1}) was stirred for 3 h, sealed in a 25 mL Teflon-lined steel autoclave, kept at 160 °C for 5 days and then slowly cooled to room temperature. Purple block crystals were collected by filtration, washed with distilled water and dried in air at ambient temperature. Yield: *ca.* 24% (based on $Na_{10}[A\text{-}\alpha\text{-}SiW_9O_{34}]\cdot 18H_2O$). Anal. calcd. (found %) for $C_{18}H_{96}Cu_3N_{12}O_{94}Si_2W_{22}Y_2$ (**1**): C 3.35 (3.43), H 1.50 (1.68), N 4.51 (4.44). Though $Na_{10}[A\text{-}\alpha\text{-}SiW_9O_{34}]\cdot 18H_2O$ was employed during the course of preparing **1**, the $[\alpha\text{-}SiW_{11}O_{39}]^{8-}$ segment is observed in **1**. Nevertheless, when Na_{10} $[A\text{-}\alpha\text{-}SiW_9O_{34}]\cdot 18H_2O$ was replaced by $K_8[\alpha\text{-}SiW_{11}O_{39}]\cdot 13H_2O$ under the similar conditions, **1** can be not obtained, which indicates that the conversion of $[A\text{-}\alpha\text{-}SiW_9O_{34}]^{10-}\rightarrow[\alpha\text{-}SiW_{11}O_{39}]^{8-}$ plays an important role in the formation of **1**. This conversion has been previously encountered in the preparations of $\{[Cu(en)_2(H_2O)][(Cu(en)(OH))_3RE(SiW_{11}O_{39})(H_2O)]\}_2\cdot 20H_2O$ ($RE = La^{III}$, Gd^{III}, Eu^{III}) and $[Cu(en)_2H_2O]_3[(\alpha\text{-}SiW_{11}O_{39})RE(H_2O)(\eta^2,\mu\text{-}1,1\text{-}CH_3COO]$ ($RE = Nd^{III}$, Sm^{III}) [27,29].

Single-crystal X-ray diffraction [33] indicates that **1** crystallizes in the triclinic space group *P*–1 and its molecular structural unit (Fig. 1a) consists of two identical mono-Y^{III} substituted Keggin-type $[\alpha\text{-}SiW_{11}O_{39}Y(H_2O)_2]^{5-}$ moieties, one bridging $[Cu(dap)_2]^{2+}$ cation, two pendant $[Cu(dap)_2(H_2O)]^{2+}$ cations, four protons and ten lattice water molecules. Bond valence sum (BVS) calculations [34] suggest that all W, Cu, and Y atoms are in the +6, +2 and +3 oxidation state in **1**, respectively. To balance of the charge of **1**, four protons should be added to the molecular structural unit. In order to localize possible binding sites of four protons, BVS calculations have been also performed on all the oxygen atoms of the POM framework (Table S1). The results show that the BVS values (1.46, 1.46, 1.50, 1.50) of O14, O14A, O26 and O26A are significantly lower than 2, indicating that four oxygen atoms may be monoprotonated. So, the structural unit of **1** is described as $[Cu(dap)_2(H_2O)]_2\{Cu(dap)_2[\alpha\text{-}H_2SiW_{11}O_{39}Y(H_2O)_2]_2\}\cdot 10H_2O$. In **1**, the $Y1^{3+}$ cation is implanted to the vacant site of the $[\alpha\text{-}SiW_{11}O_{39}]^{8-}$ fragment and exhibits a distorted monocapped trigonal antiprism

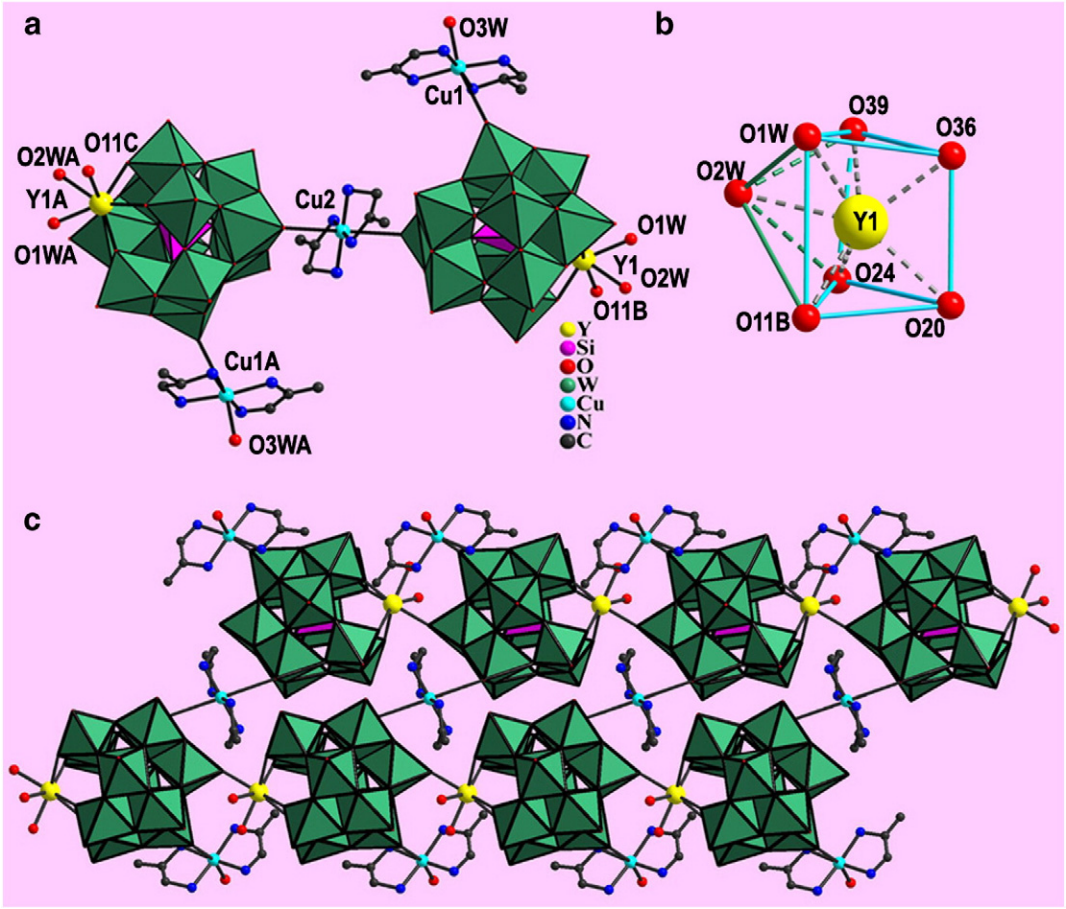

Fig. 1. (a) Ball-and-stick/polyhedral representation of the molecular structural unit of **1** with the selected labeling scheme. Lattice water molecules, protons and hydrogen atoms attached to carbon and nitrogen atoms are omitted for clarity. The atoms with the suffixes A, B and C are generated by the symmetry operation. A: $4-x, 2-y, -z$; B: $-1+x, y, z$; C: $5-x, 2-y, -z$. (b) The monocapped trigonal prism coordination geometry of the $Y1^{3+}$ cation. (c) The 1-D double-chain structure of **1**.

geometry (Fig. 1b). The $Y1^{3+}$ cation is coordinated by seven oxygen atoms, two of which are from water ligands [Y–O: 2.31(4)–2.49(4) Å], four from one $[\alpha\text{-}SiW_{11}O_{39}]^{8-}$ subunit [Y–O: 2.22(4)–2.38(3) Å] and one from the other $[\alpha\text{-}SiW_{11}O_{39}]^{8-}$ subunit on the neighboring molecular structural unit [Y–O: 2.34(4) Å]. In the $Y1^{3+}$ coordination sphere, O1W, O11B, O24, O39 group, O20, O24, O39, O36 group and O20, O11B, O1W, O36 group constitute three side surfaces of the trigonal prism and their standard deviations are 0.0893, 0.0382 and 0.0345 Å, respectively. The distances between the $Y1^{3+}$ ion and three side surfaces are 0.7523, 1.0889 and 0.6934, respectively. O2W occupies the 'cap' position over the side surface defined by O1W, O11B, O24, O39 group and the distance between O2W and the side surface is 1.6848 Å. Owing to the existence of the octahedral Cu^{II} ions in **1**, the evident Jahn–Teller effect occurs and leads to the elongation of the Cu–O bonds in the crystal field [35], as a result, the weak Cu–O bonds are considered in the discussion of the coordination geometry. The pendant $[Cu1(dap)_2(H_2O)]^{2+}$ cation grafts to the POM subunit through a terminal oxygen atom and inhibits in a distorted octahedral geometry, in which four nitrogen atoms from two dap ligands occupy the basal plane [Cu–N: 2.02(5)–2.08(3) Å] and a terminal oxygen atom [Cu–O: 3.166(28) Å] and a water oxygen atom [Cu–O: 2.349(38) Å] stand on the axial positions. The bridging $[Cu2(dap)_2]^{2+}$ cation is located on the special site with the atomic coordinate of (2, 1, 0) leading to an occupancy of 50% and employs the elongated octahedral environment with four nitrogen atoms from two dap ligands [Cu–N: 1.996(11)–2.000(11) Å] in the equatorial plane and two oxygen atoms from two adjacent $[\alpha\text{-}SiW_{11}O_{39}]^{8-}$ subunits [Cu–O: 3.209(46) Å] occupying two apical positions. As mentioned above, both $[Cu1(dap)_2(H_2O)]^{2+}$ and $[Cu2(dap)_2]^{2+}$ cations utilize the elongated octahedra, indicating that Cu1 and Cu2 cations adopt the electron configuration of $(t_{2g})^6(d_{z2})^2(d_{x2\text{-}y2})^1$.

Notably, the most interesting structural feature of **1** is that adjacent structural units are interconnected together through doubly W–O–Ce–O–W connectors giving rise to the beautiful 1-D double-chain architecture (Fig. 1c). So far as we know, **1** represents the first organic–inorganic hybrid 1-D double-chain Cu^{II}–Y^{III} heterometallic POM albeit an organic–inorganic hybrid Sm^{III}-containing 1-D double-chain germanotungstate $[Sm_2(\alpha\text{-}GeW_{11}O_{39})(DMSO)_3(H_2O)_6]^{2-}$ [36] and an inorganic Cr^{III}–La^{III} heterometallic 1-D double-chain silicotungstate $[(\gamma\text{-}SiW_{10}O_{36})_2(Cr(OH)(H_2O))_3(La(H_2O)_7)_2]^{4-}$ [37] have been reported. Comparing **1** with $[Sm_2(\alpha\text{-}GeW_{11}O_{39})(DMSO)_3(H_2O)_6]^{2-}$ [36], four evident differences are observed albeit some similarities exist: (a) the former was synthesized by the trivacant $[A\text{-}\alpha\text{-}SiW_9O_{34}]^{10-}$ precursor under hydrothermal conditions while the latter was prepared by the monovacant $[\alpha\text{-}GeW_{11}O_{39}]^{8-}$ precursor in the conventional aqueous solution; (b) the former is an organic–inorganic hybrid 1-D double-chain POM-based TRHD while the latter is an organic–inorganic hybrid 1-D double-chain Sm-containing POM; (c) the 1-D double-chains in the former are bridged by $[Cu(en)_2]^{2+}$ connectors whereas the 1-D double-chains in the latter are combined by $[Sm(DMSO)_2(H_2O)_2]^{3+}$ linkers; (d) dap ligands chelate the copper ions in the former, however, DMSO ligands coordinate to the samarium ions in the latter. In comparison with **1**, three evident distinctions are seen in $[(\gamma\text{-}SiW_{10}O_{36})_2(Cr(OH)(H_2O))_3(La(H_2O)_7)_2]^{4-}$ [37]: (a) it was synthesized by means of the preformed $Cs_{10}[(\gamma\text{-}SiW_{10}O_{36})_2(Cr(OH)(H_2O))_3]\cdot 17H_2O$ precursor in the conventional aqueous solution; (b) it is an inorganic 1-D double-chain POM-based TRHD; (c) its 1-D double-chains are joined via $[La(H_2O)_7]^{3+}$ cations. Obviously, the occurrence of these neotype 1-D double-chain POMs enrich the structural chemistry of POMs. In addition, 1-D double-chains of **1** are regularly aligned in the –AAA– mode in the *bc* plane and lattice water molecules occupy the space (Fig. 2). Provided that considering hydrogen-bonding interactions between nitrogen atoms of dap components and surface oxygen atoms of POM units or water molecules, the supramolecular architecture of **1** can be formed, in which nitrogen atoms of dap ligands work as proton donors and surface oxygen atoms of POM units and water molecules act as proton acceptors. The N–H···O distances are in the range of 2.71(5)–3.37(5) Å. These N—H···O hydrogen bonds may further enhance cohesion of the structure.

The IR spectrum of **1** has been collected from a solid sample pelletized with KBr in the range of 400–4000 cm^{-1} (Fig. S1) and displays four characteristic vibration bands resulting from the Keggin-type POM framework at 951, 888, 808, and 705 cm^{-1}, which are assigned to $\nu(W\text{–}O_t)$, $\nu(Si\text{–}O_a)$, $\nu(W\text{–}O_b)$ and $\nu(W\text{–}O_c)$, respectively [38]. In comparison with $K_8[\alpha\text{-}SiW_{11}O_{39}]\cdot 13H_2O$ (Fig. S2), the $\nu_{as}(W\text{–}O_t)$ vibration band for **1** has a red-shift of 14 cm^{-1}, the possible major reason for which may be that Y^{III} cations, $[Cu(dap)_2(H_2O)]^{2+}$ and $[Cu(dap)_2]^{2+}$ cations have strong interactions to the terminal oxygen atoms of the $[\alpha\text{-}SiW_{11}O_{39}]^{8-}$ fragments, impairing the W—O_t bonds, reducing the W—O_t bond force constant and leading to decreasing of the W—O_t vibration frequency [38]. Apparently, the IR spectrum of **1** greatly differs from that of $Na_{10}[A\text{-}\alpha\text{-}SiW_9O_{34}]\cdot 18H_2O$ (Fig. S3), which further indicates the evolution of $[A\text{-}\alpha\text{-}SiW_9O_{34}]^{10-}$ to $[\alpha\text{-}SiW_{11}O_{39}]^{8-}$ in the formation of **1**. The $\nu(NH_2)$ and $\nu(CH_2)$ stretching vibration resonances are observed at 3261 and 2959 cm^{-1} whereas the $\delta(NH_2)$ and $\delta(CH_2)$ bending vibration signals appear at 1586 cm^{-1} and 1459 cm^{-1}, which

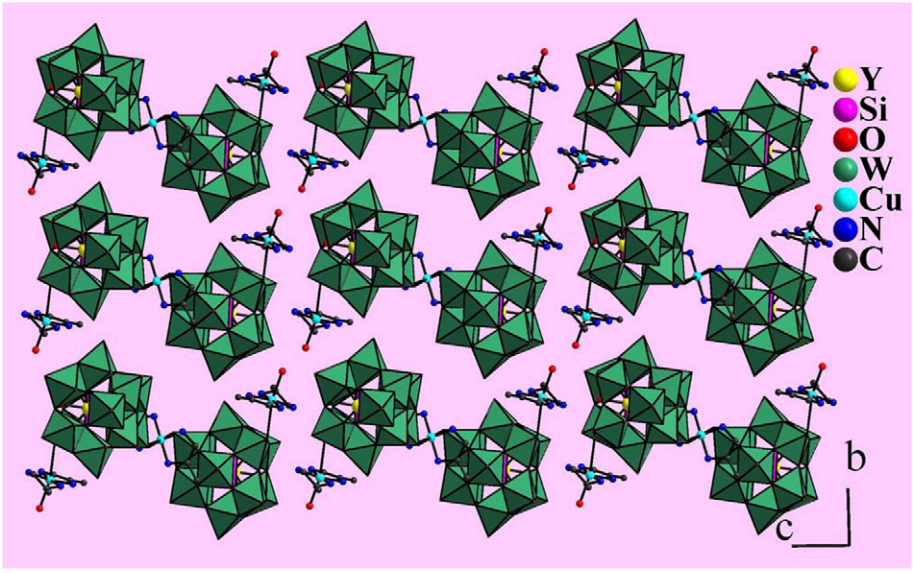

Fig. 2. The alignment of 1-D double chains of **1** showing the –AAA– mode across the *bc* plane.

confirm the existence of dap ligands in **1**. The vibration band centered at 3483 cm^{-1} is indicative of the presence of lattice water molecules or coordination water molecules. In a word, the results of IR spectrum well coincide with those of X-ray diffraction structural analysis. The UV spectrum of **1** performed in aqueous solution in the range of 190–400 nm has been recorded at room temperature (Fig. S4) and reveals only one broad lower energy absorption band centered at 251 nm, which is assigned to the pπ–dπ charge–transfer transitions of the $O_{b(c)} \rightarrow W$ bonds. However, the higher energy absorption band attributed to the pπ–dπ charge–transfer transitions of the $O_t \rightarrow W$ bonds is blue-shifted to the near UV region that is lower than 190 nm, which may be related to the coordination of Y^{III} cations and/or Cu^{II}-dap complexes to POM matrixes.

Thermogravimetry–differential thermal analysis (TG–DTA) of **1** has been measured on the crystalline sample under N_2 atmosphere from 25 to 750 °C (Fig. 3). The TG curve indicates that **1** loses weight in two steps. The weight loss of 3.87% in the first step from 25 to 140 °C corresponds to the loss of ten lattice water molecules and four coordination water molecules (calcd. 3.91%). In the corresponding DTA curve, there are two endothermal peaks at 40 and 86 °C resulting from the removal of lattice water and coordination water molecules. Above 140 °C, the second weight loss of 8.05% up to 750 °C is assigned to the removal of the remaining two coordination water molecules, six dap ligands and the dehydration of four protons (calcd. 8.01%). In the corresponding DTA curve, there is an endothermal peak at 414 °C resulting from the removal of coordination water, protons and dap ligands while a strong exothermic peak observed at 710 °C is attributed to the combustion of dap components and the collapse of the POM framework according to the West theory on decomposition of polyoxoanions [39]. The observed experimental values are in good agreement with the theoretical values.

In conclusion, a unique organic–inorganic hybrid 1-D double-chain ST-based TRHD **1** have been hydrothermally synthesized and structurally characterized. **1** adopts the novel 1-D double-chain architecture formed by dimeric Cu^{II}–Y^{III} heterometallic silicotungstate units by means of the bridging role of Y^{III} cations and it exemplifies a new type of organic–inorganic hybrid 1-D double-chain POM-based TRHD. Further work in this area will be dedicated to prepare other POM-based TRHDs by introducing organic polycarboxylic ligands or chiral organic ligands to the reaction system. Further study of this system is under way in our lab.

Acknowledgments

This work was supported by the Natural Science Foundation of China (21101055, 21071042, 21071043), China Postdoctoral Science Foundation Funded Project (201104392, 20100470996), the Natural Science Foundation of Henan Province (122300410106, 102300410093), the Foundation of State Key Laboratory of Structural Chemistry (20120013), 2012 Young Backbone Teachers Foundation from Henan Province, the Postdoctoral Science Foundation of Henan University (BH2010003), the Foundation of Education Department of Henan Province (2009A150003, 2010B150006) and the Students Innovative Pilot Plan of Henan University (2012).

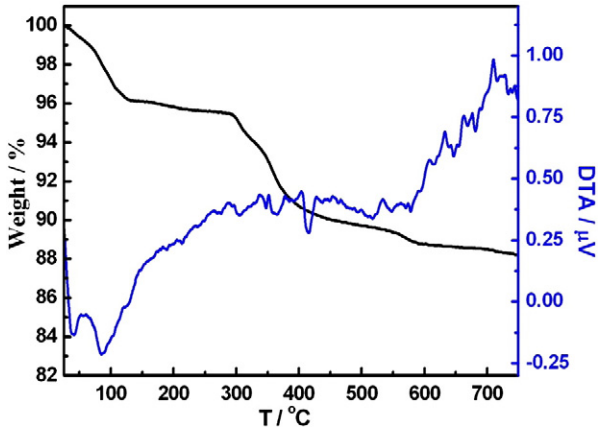

Fig. 3. TG–DTA curves of **1**.

Appendix A. Supplementary material

CCDC 896775 for **1** contains the supplementary crystallographic data for this paper. These data can be obtained free of charge from The Cambridge Crystallographic Data Centre via www.ccdc.cam.ac.uk/data_request/cif. Supplementary data associated with this article can be found in the online version at http://dx.doi.org/10.1016/j.inoche.

References

[1] A. Dolbecq, E. Dumas, C.R. Mayer, P. Mialane, Hybrid organic–inorganic polyoxometalate compounds: from structural diversity to applications, Chem. Rev. 110 (2010) 6009–6048.
[2] Z.M. Zhang, S. Yao, Y.G. Li, Y.H. Wang, Y.F. Qi, E.B. Wang, New trimeric polyoxotungstate aggregates based on $[P_2W_{12}O_{48}]^{14-}$ building blocks, Chem. Commun. (2008) 1650–1652.
[3] S.G. Mitchell, C. Streb, H.N. Miras, T. Boyd, D.L. Long, Leroy. Cronin, Face-directed self-assembly of an electronically active Archimedean polyoxometalate architecture, Nature Chem. 2 (2010) 308–312.
[4] B.S. Bassil, M. Ibrahim, R. Al-Oweini, M. Asano, Z. Wang, J. van Tol, N.S. Dalal, K.Y. Choi, R.N. Biboum, B. Keita, L. Nadjo, U. Kortz, A planar $\{Mn_{19}(OH)_{12}\}^{26+}$ unit incorporated in a 60-tungsto-6-silicate polyanion, Angew. Chem. Int. Ed. 50 (2011) 5961–5964.
[5] L.J. Chen, D.Y. Shi, J.W. Zhao, Y.L. Wang, P.T. Ma, J.P. Wang, J.Y. Niu, Three transition-metal substituted polyoxotungstates containing Keggin fragments: from trimer to one-dimensional chain to two-dimensional sheet, Cryst. Growth Des. 11 (2011) 1913–1923.
[6] V. Lahootun, C. Besson, R. Villanneau, F. Villain, L.M. Chamoreau, K. Boubekeur, S. Blanchard, R. Thouvenot, A. Proust, Synthesis and characterization of the Keggin-type ruthenium-nitrido derivative $[PW_{11}O_{39}\{RuN\}]^{4-}$ and evidence of its electrophilic reactivity, J. Am. Chem. Soc. 129 (2007) 7127–7135.
[7] F. Hussain, B.S. Bassil, L.H. Bi, M. Reicke, U. Kortz, Structural control on the nanomolecular scale: self-assembly of the polyoxotungstate wheel $[\{\beta\text{-}Ti_2SiW_{10}O_{39}\}_4]^{24-}$, Angew. Chem. Int. Ed. 43 (2004) 3485–3488.
[8] P. Mialane, A. Dolbecq, J. Marrot, E. Rivière, F. Sécheresse, A nonanuclear copper(II) polyoxometalate assembled around a μ-1,1,1,3,3,3-azido ligand and its parent tetranuclear complex, Chem. Eur. J. 11 (2005) 1771-1178.
[9] O.A. Kholdeeva, M.N. Timofeeva, G.M. Maksimov, R.I. Maksimovskaya, W.A. Neiwert, C.L. Hill, Aerobic oxidation of formaldehyde mediated by a Ce-containing polyoxometalate under mild conditions, Inorg. Chem. 44 (2005) 666–672.
[10] B.S. Bassil, M.H. Dickman, B. von der Kammer, U. Kortz, The monolanthanide-containing silicotungstates [Ln(β2-SiW11O39)2]13– (Ln = La, Ce, Sm, Eu, Gd, Tb, Yb, Lu): a synthetic and structural investigation, Inorg. Chem. 46 (2007) 2452–2458.
[11] J.W. Zhao, D.Y. Shi, L.J. Chen, X.M. Cai, Z.Q. Wang, P.T. Ma, J.P. Wang, J.Y. Niu, Two organic–inorganic hybrid 1-D and 3-D polyoxotungstates constructed from hexa-CuII substituted sandwich-type arsenotungstate units, CrystEngComm 14 (2012) 2797–2806.
[12] Z.M. Zhang, E.B. Wang, Y.F. Qi, Y.G. Li, B.D. Mao, Z.M. Su, Synthesis, characterization, and crystal structures of double-cubane-substituted and asymmetric penta-Ni-substituted dimeric polyoxometalates, Cryst. Growth Des. 7 (2007) 1305–1311.
[13] W.L. Chen, Y.G. Li, Y.H. Wang, E.B. Wang, Z.M. Zhang, A new polyoxometalate-based 3d–4f heterometallic aggregate: a model for the design and synthesis of new heterometallic clusters, Dalton Trans. 2008 (2008) 865–867.
[14] J.F. Cao, S.X. Liu, R.G. Cao, L.H. Xie, Y.H. Ren, C.Y. Gao, L. Xu, Organic–inorganic hybrids assembled by bis(undecatungstophosphate)lanthanates and dinuclear copper(II)–oxalate complexes, Dalton Trans. 2008 (2008) 115–120.
[15] X.K. Fang, P. Kögerler, PO_4^{3-}-mediated polyoxometalate supercluster assembly, Angew. Chem. Int. Ed. 47 (2008) 8123–8126.
[16] S. Yao, Z.M. Zhang, Y.G. Li, Y. Lu, E.B. Wang, Z.M. Su, Two heterometallic aggregates constructed from the $\{P_2W_{12}\}$-based trimeric polyoxotungstates and 3d–4f heterometals, Cryst. Growth Des. 10 (2010) 135–139.
[17] Y.W. Li, Y.G. Li, Y.H. Wang, X.J. Feng, Y. Lu, E.B. Wang, A new supramolecular assembly based on triple-Dawson-type polyoxometalate and 3d–4f heterometallic cluster, Inorg. Chem. 48 (2009) 6452–6458.
[18] S. Reinoso, M. Giménez-Marqués, J.R. Galán-Mascarós, P. Vitoria, J.M. Gutiérrez-Zorrilla, Giant crown-shaped polytungstate formed by self-assembly of Ce^{III}-stabilized dilacunary Keggin fragments, Angew. Chem. Int. Ed. 49 (2010) 8384–8388.
[19] X. Feng, W. Zhou, Y. Li, H. Ke, J. Tang, R. Clérac, Y. Wang, Z. Su, E. Wang, Polyoxometalate-supported 3d–4f heterometallic single-molecule magnets, Inorg. Chem. 51 (2012) 2722–2724.

[20] D.Y. Shi, L.J. Chen, J.W. Zhao, Y. Wang, P.T. Ma, J.Y. Niu, Two novel 2D organic–inorganic hybrid lacunary Keggin phosphotungstate 3d–4f heterometallic derivatives: $[Cu(en)_2]_2H_6[Ce(\alpha\text{-}PW_{11}O_{39})_2]\cdot 8H_2O$ and $[Cu(dap)_2(H_2O)][Cu(dap)_2]_{4.5}[Dy(\alpha\text{-}PW_{11}O_{39})_2]\cdot 4H_2O$, Inorg. Chem. Commun. 14 (2011) 324–329.
[21] J.Y. Niu, S.W. Zhang, H.N. Chen, J.W. Zhao, P.T. Ma, J.P. Wang, 1-D, 2-D and 3-D organic–inorganic hybrids assembled from Keggin-type polyoxometalates and 3d−4f heterometals, Cryst. Growth Des. 11 (2011) 3769–3777.
[22] J.W. Zhao, D.Y. Shi, L.J. Chen, Y.Z. Li, P.T. Ma, J.P. Wang, J.Y. Niu, Novel polyoxometalate hybrids consisting of copper–lanthanide heterometallic / lanthanide germanotungstate fragments, Dalton Trans. 41 (2012) 10740–10751.
[23] A. Merca, A. Müller, J.V. Slageren, M. Läge, B. Krebs, Systematic study of the interaction between V^{IV} centres and lanthanide ions M^{III} in well defined $\{V^{IV}{}_2M^{III}\}\{As^{III}W_9O_{33}\}_2$ sandwich type clusters: Part 1, J. Clust. Sci. 18 (2007) 711–719.
[24] W.L. Chen, Y.G. Li, Y.H. Wang, E.B. Wang, An inorganic aggregate based on a sandwich-type polyoxometalate with lanthanide and potassium cations: from 1D chiral ladder-like chains to a 3D open framework, Eur. J. Inorg. Chem. 2007 (2007) 2216–2220.
[25] Z.M. Zhang, Y.G. Li, W.L. Chen, E.B. Wang, X.L. Wang, Two-dimensional (3,6)-topological inorganic aggregate based on the sandwich-type polyoxometalate and lanthanide linkers, Inorg. Chem. Commun. 11 (2008) 879–882.
[26] Z.M. Zhang, Y.G. Li, S. Yao, E.B. Wang, Hexameric polyoxometalates decorated by six 3d–4f heterometallic clusters, Dalton Trans. 40 (2011) 6475–6479.
[27] B. Nohra, P. Mialane, A. Dolbecq, E. Rivière, J. Marrot, F. Sécheresse, Heterometallic 3d–4f cubane clusters inserted in polyoxometalate matrices, Chem. Commun. 2009 (2009) 2703–2705.
[28] J.D. Compain, P. Mialane, A. Dolbecq, I.M. Mbomekallé, J. Marrot, F. Sécheresse, C. Duboc, E. Rivière, Structural, magnetic, EPR, and electrochemical characterizations of a spin-frustrated trinuclear Cr^{III} polyoxometalate and study of its reactivity with lanthanum cations, Inorg. Chem. 49 (2010) 2851–2858.
[29] D.Y. Du, J.S. Qin, S.L. Li, Y.A. Lan, X.L. Wang, Z.M Su, 3d–4f heterometallic complexes for the construction of POM-based inorganic–organic hybrid compounds: from manoclusters to one-dimensional ladder-like chains, Aust. J. Chem. 63 (2010) 1389–1395.
[30] S.W. Zhang, J.W. Zhao, P.T. Ma, H.N. Chen, J.Y. Niu, J.P. Wang, Organic–inorganic hybrids based on monovacant Keggin-type silicotungstates and 3d–4f heterometals, Cryst. Growth Des. 12 (2012) 1263–1272.
[31] S.W. Zhang, J.W. Zhao, P.T. Ma, J.Y. Niu, J.P. Wang, Rare-earth–transition-metal organic–inorganic hybrids based on Keggintype polyoxometalates and pyrazine-2,3-dicarboxylate, Chem. Asian J. 7 (2012) 966–974.
[32] J. Luo, C.L. Leng, L.J. Chen, J. Yuan, H.Y. Li, J.W. Zhao, Three 3D organic–inorganic hybrid heterometallic polyoxotungstates assembled from 1:2-type $[Ln(\alpha\text{-}SiW_{11}O_{39})_2]^{13-}$ silicotungstates and $[Cu(dap)_2]^{2+}$ linkers, Synthetic Met. 162 (2012) 1558–1565.
[33] Crystal data for 1: C18H96Cu3N12O94Si2W22Y2, Mr = 6454.39, triclinic, space group P–1, a = 11.390(11), b = 12.568(11), c = 21.316(19) Å, α = 85.202(15), β = 75.231(19), γ = 74.379(16) ° V = 2841(4) Å3, Z = 1, Dc = 3.772 g·cm–3, μ = 23.845 mm–1, F(000) = 2861, GOOF = 1.093. Of 13682 total reflections collected, 9728 were unique (Rint = 0.0916), R1(wR2) = 0.1136 (0.2344) for 591 parameters and 4251 reflections [I > 2σ(I)]. Intensity data were collected on a Bruker Smart APEX II CCD diffractometer with graphite-monochromated Mo Kα radiation (λ = 0.71073 Å) at 296(2) K. The structure was solved by direct methods and refined by full-matrix least squares on F2 using the SHELXTL–97 program package. Intensity data were corrected for Lorentz and polarization effects as well as for multi-scan absorption. All of the non-hydrogen atoms were refined anisotropically. Positions of the hydrogen atoms attached to the carbon and nitrogen atoms were geometrically placed. All hydrogen atoms were refined isotropically as a riding mode using the default SHELXTL parameters.
[34] I.D. Brown, D. Altermatt, Bond-valence parameters obtained from a systematic analysis of the inorganic crystal structure database, Acta Cryst. B41 (1985) 244–247.
[35] J.W. Zhao, S.T. Zheng, G.Y. Yang, 0-D and 1-D inorganic–organic composite polyoxotungstates constructed from in-situ generated monocopper^{II}-substituted Keggin polyoxoanions and copper^{II}–organoamine complexes, J. Solid State Chem. 181 (2008) 2205–2216.
[36] J.P. Wang, X.Y. Duan, X.D. Du, J.Y. Niu, Novel rare earth germanotungstates and organic hybrid derivatives: synthesis and structures of $M/[\alpha\text{-}GeW_{11}O_{39}]$ (M = Nd, Sm, Y, Yb) and $Sm/[\alpha\text{-}GeW_{11}O_{39}](DMSO)$, Cryst. Growth Des. 6 (2006) 2266–2270.
[37] J.D. Compain, P. Mialane, A. Dolbecq, I.M. Mbomekallé, J. Marrot, F. Sécheresse, C. Duboc, E. Rivière, Structural, magnetic, EPR, and electrochemical characterizations of a spin-frustrated trinuclear Cr^{III} polyoxometalate and study of its reactivity with lanthanum cations, Inorg. Chem. 49 (2010) 2851–2858.
[38] J.P. Wang, J.W. Zhao, X.Y. Duan, J.Y. Niu, Syntheses and structures of one- and two-dimensional organic–inorganic hybrid rare earth derivatives based on monovacant Keggin-type polyoxotungstates, Cryst. Growth Des. 6 (2006) 507–513.
[39] S.F. West, L.F. Audrieth, Differential thermal analysis of some heteropoly acids of molybdenum and tungsten, J. Phys. Chem. 59 (1955) 1069–1072.